AD-A047 016 AERONAUTICAL RESEARCH LABS MELBOURNE (AUSTRALIA) F/G 11/6
MECHANISMS OF STRESS-CORROSION CRACKING AND LIQUID-METAL EMBRIT--ETC(U)
FEB 77 S P LYNCH

UNCLASSIFIED ARL/MAT.101 NL

1 OF 1
ADA047 016

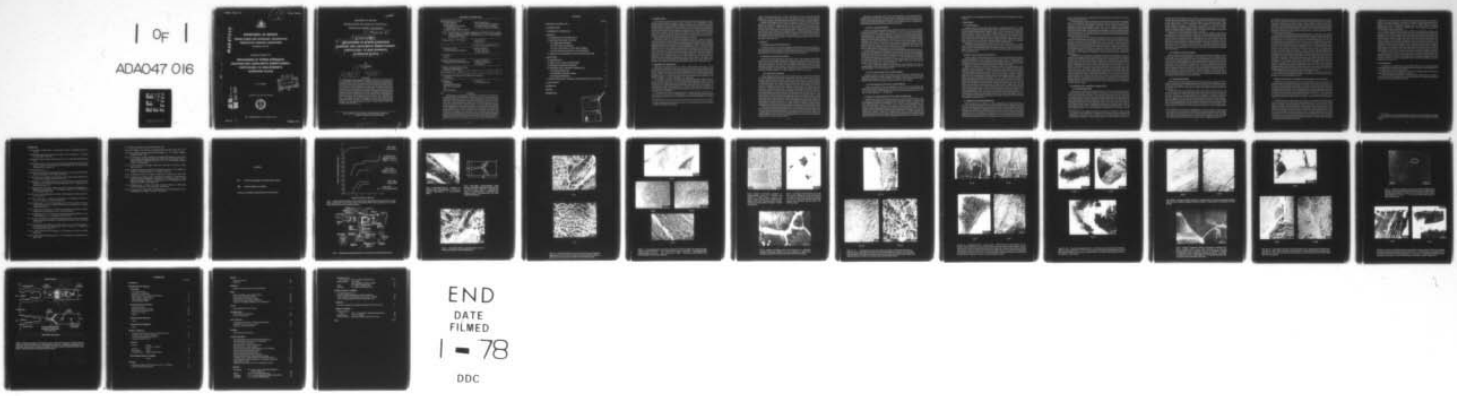

END
DATE FILMED
1 - 78
DDC

ARL/Mat. Report 101

AR No. 000-234

DEPARTMENT OF DEFENCE

DEFENCE SCIENCE AND TECHNOLOGY ORGANISATION

AERONAUTICAL RESEARCH LABORATORIES

MELBOURNE, VICTORIA

MATERIALS REPORT 101

MECHANISMS OF STRESS-CORROSION CRACKING AND LIQUID-METAL EMBRITTLEMENT, PARTICULARLY IN HIGH-STRENGTH ALUMINIUM ALLOYS

S. P. LYNCH

Approved for Public Release

COPY No 17

February 1977

AR No. 234

DEPARTMENT OF DEFENCE

DEFENCE SCIENCE AND TECHNOLOGY ORGANISATION

AERONAUTICAL RESEARCH LABORATORIES

(14) ARL/MAT. 101

(9) MATERIALS REPORT 101

(6) # MECHANISMS OF STRESS-CORROSION CRACKING AND LIQUID-METAL EMBRITTLEMENT, PARTICULARLY IN HIGH-STRENGTH ALUMINIUM ALLOYS.

by

(10) S. P. LYNCH

(11) Feb 77 (12) 27 p.

SUMMARY

Metallographic and fractographic observations of sub-critical crack growth in a precipitation-hardened Al-Zn-Mg alloy in liquid-metal, aqueous, and water-vapour/air environments suggest that stress-corrosion cracking and liquid-metal embrittlement in this alloy involve a common mechanism. Sub-critical crack growth in all these environments can produce entirely dimpled fracture surfaces and, in liquid-metal and aqueous environments, crack growth can occur extremely rapidly. It is proposed that stress-corrosion cracking and liquid-metal embrittlement in aluminium alloys (and possibly other materials) can be explained on the basis that chemisorption of environmental species facilitates nucleation of dislocations at crack tips. Such a process would produce sub-critical crack growth with less blunting at crack tips than in inert environments and, hence, would explain observations that dimples on fracture surfaces after SCC are smaller and shallower than those on overload fractures. The results suggest that neither dissolution nor hydrogen-embrittlement processes occurred during stress-corrosion cracking in aluminium alloys.

POSTAL ADDRESS: Chief Superintendent, Aeronautical Research Laboratories, Box 4331, P.O., Melbourne, Victoria, 3001, Australia.

008 650

DOCUMENT CONTROL DATA

Security classification of this page

1. Document Numbers
   (a) AR Number: 234
   (b) Document Series and Number: Materials Report 101
   (c) Report Number: ARL Mat. Rpt 101

2. Security Classification
   (a) Complete document: Unclassified
   (b) Title in isolation: Unclassified
   (c) Summary in isolation: Unclassified

3. Title: MECHANISMS OF STRESS-CORROSION CRACKING AND LIQUID-METAL EMBRITTLEMENT PARTICULARLY IN HIGH-STRENGTH ALUMINIUM ALLOYS

4. Personal Author: S. P. LYNCH

5. Document Date: February 1977

6. Type of Report and period covered:

7. Corporate Author(s): Aeronautical Research Laboratories

8. Reference Numbers
   (a) Task: AIR 72/08
   (b) Sponsoring Agency:

9. Cost Code: 35 1610

10. Imprint (Publishing establishment): Aeronautical Research Laboratories 1977

11. Computer Program(s) (Title(s) and language(s)): Not applicable

12. Release Limitations (of the document)
Approved for Public Release

12-0. Overseas: No.		P.R.	1	A		B		C		D		E	

13. Announcement Limitations (of the information on this page):
No Limitation

14. Descriptors:
Embrittlement
Liquid-metal embrittlement
Aluminium, Metallography
Tin
Zinc, Fractography

15. Cosati Codes:
1113, 1106, 1407, 1402

16. *SUMMARY*

Metallographic and fractographic observations of sub-critical crack growth in a precipitation-hardened Al-Zn-Mg alloy in liquid-metal, aqueous, and water-vapour/air environments suggest that stress-corrosion cracking and liquid-metal embrittlement in this alloy involve a common mechanism. Sub-critical crack growth in all these environments can produce entirely dimpled fracture surfaces and, in liquid-metal and aqueous environments, crack growth can occur extremely rapidly. It is proposed that stress-corrosion cracking and liquid-metal embrittlement in aluminium alloys (and possibly other materials) can be explained on the basis that chemisorption of environmental species facilitates nucleation of dislocations at crack tips. Such a process would produce sub-critical crack growth with less blunting at crack tips than in inert environments and, hence, would explain observations that dimples on fracture surfaces after SCC are smaller and shallower than those on overload fractures. The results suggest that neither dissolution nor hydrogen-embrittlement processes occurred during stress-corrosion cracking in aluminium alloys.

CONTENTS

1. INTRODUCTION

Stress-corrosion cracking (SCC) and liquid-metal embrittlement (LME) refer to environmentally assisted initiation and growth of cracks; references 1–3 give comprehensive reviews. Fractures produced by SCC and LME are generally associated with less deformation and often with fracture paths and modes different from those in inert environments. The most important variables affecting susceptibility to SCC and LME are (i) alloy composition/strength/microstructure, (ii) composition of the environment†, (iii) temperature, (iv) level of applied stress/stress mode, and (v), for SCC, electrode potential. The effects of stress intensity on rates of crack growth of two aluminium alloys in various environments are shown in Fig. 1 as an example[4]. A schematic summary of the many effects which may be involved in SCC is shown in Fig. 2[5]; in the case of LME, generally only adsorption reactions are involved.

Most theories of SCC[2-4] are based on electrochemical reactions at crack tips. Proposals include (i) stress/strain assisted dissolution, (ii) repeated steps of film rupture by slip, dissolution, repassivation, and (iii) corrosive attack (tunneling) along active slip planes or regions of chemical segregation followed by mechanical rupture of remaining ligaments. Another commonly suggested mechanism of SCC involves diffusion of environmental species (eg. H^+, Cl^-) into the metal lattice ahead of crack tips, resulting in embrittlement of this material; hydride formation may occur in some cases. It has been proposed[1] that LME is due to chemisorption of liquid-metal atoms which reduce the strength of interatomic bonds at crack tips so that tensile rupture of bonds occurs at low applied stresses; it has also been suggested[6, 7] that this explanation is applicable to SCC. All the above theories, and combinations of them, have been proposed to explain SCC in high-strength Al-Zn-Mg alloys, such as those studied in the present work; the aim of the present metallographic and fractographic studies was to gain a better understanding of the mechanisms of environmentally induced crack growth in aluminium alloys.

2. EXPERIMENTAL PROCEDURE

High purity Al-Zn-Mg (6·27 wt.% Zn, 2·94 wt.% Mg) specimens were solution-treated at 430°C (in salt), quenched in boiling water, aged at 100°C for (A) 2 min and (B) 60 min, and then at 180°C (in oil) for 120 min. These heat treatments produce fine dispersions of precipitates in grain interiors, coarser dispersions of larger precipitates at grain boundaries and precipitate-free zones (PFZ's), ~0·2 μm wide in case A and ~0·05 μm wide in case B, adjacent to grain boundaries (e.g. Fig. 3). Proof stresses (and elongation to fracture) for heat treatments A and B were ~410 MPa (~8%) and ~420 MPa (~1%), respectively.

Crack growth was studied using bolt-loaded double-cantilever-beam (DCB) specimens (Fig. 4). For these specimens, at a constant crack-opening displacement (COD), the stress intensity K at the crack tip decreases with increasing crack length. Thus, fracture in dry air was produced by continuously increasing COD until pop-in occurred at Kc; specimens for LME and SCC studies were pre-cracked in dry air then, without reducing the applied load (so that K was just below Kc), liquid metal was applied†† around crack tips or specimens were immersed in SCC environments.

Environments used were (i) liquid mercury, (ii) a liquid alloy (44·7% Bi, 22·6% Pb, 19·1% In, 8·3% Sn, 5·3% Cd–wt.%) (melting point ~47°C), (iii) saturated (aqueous) potassium iodide solution, (iv) distilled water, (v) water-vapour/air at 20% relative humidity (over a saturated

† Environments which produce cracking in some materials will not necessarily do so in others.

†† Lightly scratching the surface around the crack tip after applying liquid metal facilitated 'wetting' and induced crack growth.

solution of potassium acetate, and (vi) 'inert' environments, viz. dry air (over silica gel) and paraffin oil. Tests were performed at ~50°C in the liquid alloy and at ~20°C in the other environments, except for a few tests at higher temperatures (up to 160°C) in dry air and paraffin oil.

Standard metallographic and fractographic techniques were used for examining specimens. Liquid alloy was generally removed as soon as possible after fracture by a jet of hot water followed by immersion in concentrated nitric acid for 1 min; liquid mercury was removed by evaporation in vacuum at ~100°C. Fractures were cleaned further by stripping plastic replicas from the surfaces. Experiments to show that the presence of liquid metal on, or its subsequent removal from, fracture surfaces had no significant effects on surface topography were carried out. A metallographic study to examine the effects of exposure of specimens to water-vapour/air during aging was also undertaken, since it had been reported [8, 9] that such specimens (of an Al 7% Zn 3% Mg alloy) were embrittled, compared with specimens aged in dry air, and that this effect was relevant to SCC.

3. RESULTS

3.1 Overload Fracture of Al-Zn-Mg in Dry Air

Overload crack growth was almost completely intercrystalline and, for heat-treatment A, fracture surfaces were almost entirely covered by dimples (Fig. 5); a few areas were comparatively flat, although they showed impressions of grain-boundary precipitates and possibly extremely shallow dimples. For heat-treatment B, many such flat areas were observed.

3.2 Sub-Critical Crack Growth in Al-Zn-Mg

Specimens given heat-treatment A were mainly used to study sub-critical crack growth because, for this heat-treatment, differences in fracture-surface appearance between overload, LME and SCC fractures were more marked; consequently, mechanisms of crack growth were more easily deduced from observations of these fracture surfaces than from those for heat-treatment B. Sub-critical crack growth in all environments was characterised by considerable crack-branching (Fig. 4) and, hence, simple calculations of stress intensity are ruled out. Stress intensities are therefore referred to as 'high', 'intermediate', and 'low'—see Fig. 4.

3.2.1 Liquid-Metal Environments

Wetting specimens (loaded to near Kc) with liquid mercury or liquid alloy resulted in very rapid (10–100 mm/sec) sub-critical crack growth, often until one or both arms of the specimen completely broke off (Fig. 4). In some cases, crack growth at low stress intensities was apparently discontinuous since intermittent clicking sounds, probably resulting from bursts of rapid crack growth, were audible. Fracture surfaces were almost entirely intercrystalline and, for heat-treatment A, were almost completely covered by dimples (Figs 6–11). The size and shape of dimples depended on the orientation of grain facets to the applied stress and varied even on one facet; nevertheless, it was apparent that dimples were smaller, shallower, and more elongated (in the direction of crack growth) than dimples on overload fractures, and that dimples became smaller and shallower with decreasing stress intensity (Figs 9–11). For heat-treatment B, fracture surfaces produced by LME showed many flat facets similar to those observed after overload. Wetting flat, electropolished surfaces with liquid mercury or liquid alloy (after removal of the oxide film in NaOH solution) and then removing the liquid metal, as described earlier, resulted in surfaces with the same (slightly pitted) appearance as those only only immersed in NaOH solution (Fig. 12). These observations suggest that the presence of liquid metal on surfaces after fracture has no significant effects on surface topography and that the dimples observed after LME, for heat-treatment A, are produced by the fracture process itself.

Examination of fractures *before* removing the low-melting-point alloy showed that, when there was only a small amount of liquid alloy at the crack tip during crack growth, small regions of material had fractured without being wet by the liquid metal (Fig. 13); these regions were probably ligaments of unfractured material lagging behind the main crack front. Larger, more equiaxed dimples, typical of fracture in air (heat-treatment A), were observed in these regions (compared to the rest of the fracture surface).

Deformation accompanying crack growth was observed (a) on the previously electropolished sides of specimens, and (b) in their interior, by aging after fracture (to 'decorate' dislocations), sectioning, polishing, and etching (Fig. 14). (Comparisons with undeformed specimens showed that the slip markings (Fig. 14) were a result of fracture and not a consequence of inhomogeneous precipitation during the original heat treatment).

3.2.2 SCC in Aqueous Environments

Immersion of pre-cracked specimens (heat-treatment B), loaded to near Kc, in saturated potassium iodide solution resulted in an increment ($\sim$1 mm) of very rapid crack growth ($\sim$10 mm/sec) within one second of immersion. This burst of crack growth was detected by direct observation (at $\times$50) on the polished sides of specimens and by the characteristic audible sounds emitted during rapid cracking. Fractographic observations showed that these increments of rapid crack growth occurred along most of the crack front and not just at the surface. Similar observations were made for heat-treatment A in KI solution and for heat-treatments A and B in distilled water; however, in these cases, initial crack-growth increments were shorter and/or incubation times were longer. In all cases, crack growth was subsequently discontinuous with bursts of rapid fracture separated by periods of crack arrest and/or slow crack growth; the bursts of rapid fracture were less frequent at lower stress intensities.

Fracture surfaces for heat-treatment B showed mainly flat intercrystalline facets with a few areas of shallow dimples; for heat-treatment A, intercrystalline facets were almost completely dimpled and, as for LME fractures, dimples were generally smaller, shallower and more elongated at lower stress intensities (Figs 15–26). Even at high stress intensities, dimples were much smaller and shallower than those on overload fractures (Figs 15–17). At intermediate stress intensities, very large, flat, equiaxed dimples among areas of small dimples (Figs 18–20) were observed as well as striations (Fig. 18). At low stress intensities, slightly inclined steps, running in the direction of crack growth, were common (Figs 22–25).

The extent of deformation adjacent to stress-corrosion cracks, observed on the sides of polished specimens and in their interior, decreased with decreasing stress intensity but was still quite appreciable at low stress intensities (Fig. 27).

3.2.3 SCC in Water-Vapour/Air (20% Relative Humidity)

Specimens, loaded to near Kc, showed relatively slow crack growth ($\sim 10^{-4}$mm/sec) in this environment compared to cracking in aqueous environments; bursts of rapid fracture were not observed. Fracture surfaces, for heat-treatment A at high stress intensities were almost entirely dimpled (Figs 28–30). (Crack growth at low stress intensities was not studied).

3.2.4 Sub-Critical Crack Growth in Dry Air and Paraffin Oil

At high stress intensities, in dry air and paraffin oil at 160°C, bursts of rapid cracking were observed and average crack-growth rates were about the same as those in distilled water (i.e. $1–10^{-1}$mm/sec). Rates of crack growth decreased with decreasing temperature and at 20°C were not readily detected (i.e. $< 10^{-6}$mm/sec).

3.3 Exposure of Al-Zn-Mg Specimens to Water-Vapour/Air During Aging.

A heat-treatment reported[8] to give large reductions in tensile ductility after aging in moist air (compared to the ductility after aging in dry air) was studied; specimens ($\sim$300 μm thick) were mechanically polished, solution-treated at 475°C for 30 min in argon, quenched in cold water, dried, and aged for 4 days at 70°C in moist air (100% relative humidity). This heat-treatment produced thick oxide films at the surface, with films somewhat thicker in grain-boundary regions. Progressively removing the surface by electropolishing showed that pits (slits) extended up to 20 μm into specimens along grain boundaries (Fig. 31). Some pits were observed within grains, although, in many cases, it appeared that these pits had been associated with grain boundaries but that grain-boundary migration had subsequently occurred. Intercrystalline fracture of specimens in air also revealed the pitting effect (Fig. 32) and, in addition, exposed

internal islands of an (unidentified) thin film (Fig. 33). No such effects were detected after aging in dry air.

4. DISCUSSION

4.1 Overload Fracture

Overload fracture in high-strength Al-Zn-Mg alloys is understood quite well[10-12]; crack growth involves preferential plastic deformation in PFZ's and nucleation of voids by separation of grain-boundary-precipitate/matrix interfaces ahead of cracks. Coalescence of cracks and voids then occurs by necking of the bridge of material between cracks and voids; this process involves nucleation or egress of dislocations at tips of cracks (and voids), producing crack (void) growth, with general dislocation activity resulting in blunting at crack (void) tips (Fig. 34 (a)). Wider PFZ's (and smaller area fractions of grain-boundary precipitate) allow voids to blunt to greater extents; thus, dimples on fracture surfaces are deeper and more well defined for heat-treatment A ('wide' PFZ) than for heat-treatment B ('narrow' PFZ).

Deformation accompanying crack growth occurs not only in PFZ's but also, to a lesser extent, in the precipitation-hardened grains. Slip in grain interiors concentrates in pre-existing 'quench bands' of lower precipitate density than adjacent regions and, hence, narrow, discrete bands of dislocations are often observed[10]; however, these bands should not be relevant to the basic fracture process.

4.2 Effects of Prior Corrosion on Tensile Ductility

Tensile elongation of Al-Zn-Mg specimens occurs by shearing of adjacent grains (involving concentrated deformation in PFZ's) and deformation of grain interiors, the latter making an increasing contribution to overall elongation with decreasing strength.[10-12] Deformation is accompanied by nucleation and (stable) growth of intercrystalline cracks and specimens continue to elongate until a critical crack size for rapid unstable crack growth is reached.

Exposure of specimens to corrosive environments during or after aging produces intercrystalline corrosion (eg. pitting, cracking), the severity of which depends on environment, composition, and heat-treatment.[13, 14] Such corrosion effectively pre-cracks specimens and, as would be expected, decreases tensile ductility. Swann and co-workers,[8, 9] however, attributed a decreased ductility of specimens exposed to moist air during aging (compared to specimens aged in dry air) to embrittlement by hydrogen rather than intercrystalline corrosion. The present studies, using the same experimental procedure (§3·3), but a slightly (although probably not significantly) different composition from Swann, showed that pre-exposure of specimens to moist air during aging did, in fact, produce intercrystalline pitting /cracking (Figs 31, 32). The present work also showed that grain-boundary migration/grain growth could occur such that previous intercrystalline corrosion effects were no longer at grain boundaries. Such an effect could account for observations[8] that heat-treatment of specimens after pre-exposure partially restored tensile ductility since pits within grains should be less effective than intercrystalline pits in reducing ductility. Effects of prior corrosion on ductility are obviously complex and it is considered that further work is required (a) to investigate the pitting phenomenon (Fig. 31) in more detail and to identify the intercrystalline films (Fig. 33) formed during aging in moist air, (b) to determine whether diffusion of hydrogen into specimens is important, and (c) to elucidate if these effects are relevant to SCC.

4.3 Mechanism of Liquid-Metal Embrittlement

LME can generally be attributed to an effect of chemisorption of liquid-metal atoms at crack tips since (a) rates of crack growth in embrittling liquid-metal environments are extremely fast, and (b) mutual solubilities of solid and liquid metals are often negligible; thus, other processes such as diffusion of embrittling metal atoms ahead of crack tips or stress-assisted dissolution at crack tips can usually be discounted. In the past, it has been assumed[1] that chemisorption lowers the tensile strength of interatomic bonds at crack tips, without significantly affecting the shear stress required to move dislocations, so that crack growth occurs by repeated adsorption and breaking of bonds at low applied stress. Fracture surfaces produced by such a

process would be flat, little if any deformation would be associated with fracture, and blunting at crack tips would not occur.

The present studies of LME in Al-Zn-Mg show that dimpled fracture surfaces are produced (Figs 6–11) indicating that microvoids nucleate and grow ahead of cracks and that some blunting does occur at crack tips. Metallographic observations showing appreciable deformation in precipitation-hardened grains adjacent to cracks (Fig. 14) also suggested that considerable deformation occurred in PFZ's during fracture. (A recent study[15] of LME in aluminium single crystals and other pure metals also showed extensive slip adjacent to cracks and dimpled fracture surfaces in many cases.) It is concluded, therefore, that crack growth in embrittling liquid-metal environments generally occurs by plastic flow (shear movement of atoms) rather than by tensile separation of atoms at crack tips.

It has been proposed[15] that LME can be explained on the basis that chemisorption of liquid-metal atoms facilitates the nucleation of dislocations at crack tips. Atoms at metal surfaces/crack tips, in vacuum, have fewer neighbours than atoms in the interior and hence the lattice spacings in the first few atomic layers differ from those in the interior[16]. This perturbation of the lattice at the surface should hinder the nucleation (and egress) of dislocations at surfaces[17] since dislocations moving in the first few atomic layers would be associated with larger-than-normal lattice distortions. Chemisorption of liquid-metal atoms on surfaces effectively increases the number of neighbours surrounding surface atoms and should reduce the 'surface-lattice distortion'.[18] Thus, nucleation of dislocations at surfaces (crack tips) could be facilitated by chemisorption.

Adsorption-activated nucleation (and subsequent movement) of dislocations at crack tips would not only produce sub-critical crack growth by shear but would also explain observations that dimples on LME fractures are shallower than dimples on overload fractures, i.e. less blunting occurs at crack tips during crack growth in liquid-metal environments. Blunting involves general dislocation activity (a general strain) around crack tips and usually requires slip on at least five independent slip systems, cross-slip, and interpenetration of dislocations.[19] Crack growth, on the other hand, can occur by slip (alternate shear) on only two slip planes intersecting crack tips.[20] The balance between crack growth and crack-tip blunting (both relax elastic-strain energy around cracks) should therefore be determined by the relative proportions of slip on planes intersecting crack tips compared to 'general' slip ahead of cracks; larger proportions of the former, which is promoted by chemisorption, favour crack growth and reduce crack-tip blunting.† Less 'general' slip should occur at lower stress intensities; thus, dimples become shallower with decreasing stress intensity (Figs 9–11). Dimples on LME fractures are generally elongated in the direction of crack growth (on both fracture surfaces) since adsorption-activated slip occurs only at external crack tips and, hence, external cracks grow preferentially towards voids (Fig. 34(b)).

4.4 Mechanisms of SCC, particularly in Aluminium Alloys

4.4.1 Adsorption-induced Slip

Chemisorption of species other than liquid-metal atoms (e.g. water molecules) could reduce 'surface-lattice distortion', facilitate nucleation of dislocations at crack tips, and produce sub-critical crack growth. Several workers[6, 7] have previously proposed that SCC and LME occur by a common mechanism since there are many similarities between the two processes. Specificity of environment, greater cracking susceptibility of higher strength alloys, and cleavage-like and brittle intercrystalline fractures are characteristic of both SCC and LME. The formation of cleavage-like {100} fracture surfaces during SCC/LME in 'normally' ductile FCC materials (e.g. aluminium single crystals in liquid-metal environments[15], austenitic stainless steels in boiling $MgCl_2$ solution[2]) can be explained by adsorption-induced alternate shear on {111} slip planes intersecting crack tips.[15] In Al-Zn-Mg (for heat-treatment A), both SCC and LME

† Chemisorption can only influence the first few atomic layers at surfaces of metals and the stress required to move dislocations on slip planes not intersecting crack tips/surfaces will be unaffected by chemisorption. Thus, adsorption does not generally influence the 'bulk' flow characteristics of specimens. A more detailed discussion of LME is given in reference 15.

produce almost entirely dimpled fracture surfaces, with dimples generally becoming smaller and shallower with decreasing stress intensity. Adsorption-activated nucleation of dislocations can also explain these observations, as discussed above. The very rapid initial rates of crack growth† observed within < 1 sec. of immersion of Al-Zn-Mg specimens in KI solution (§3.2.2) strongly suggest that adsorption is responsible; other processes, e.g. dissolution, oxide-film formation, diffusion of hydrogen ahead of cracks, probably do not have time to occur. Observations of corrosion-fatigue in aluminium alloys[21] also suggest that adsorption at crack tips, rather than diffusion of hydrogen ahead of cracks, is involved.

Objections to a common mechanism of SCC and LME (and, implicitly, to SCC due to adsorption) have been raised in the past[2,3] because (a) it was then assumed that LME occurred by tensile separation of atoms ('decohesion') at crack tips and, (b) it was considered that a 'decohesion' process was inapplicable to SCC—appreciable slip was known to occur at crack tips during SCC. The present studies show that considerable slip occurs during both SCC and LME; both processes can be explained by adsorption-induced slip and, hence, such objections are not appropriate. For SCC, dissolution, oxide-film formation, or hydrogen embrittlement (discussed below), could occur in conjunction with (and, in some cases, instead of) adsorption-induced crack growth—the precise behaviour will depend on the alloy, environment, stress-intensity and other variables.

4.4.2 Dissolution, Oxide-Film Formation

Many previously proposed mechanisms of SCC have been based on dissolution processes at crack tips. However, dissolution appears to be unnecessary for SCC in aluminium alloys since (i) SCC occurs in water-vapour/air at very low relative humidities; here, dissolution cannot occur since there is no liquid electrolyte at crack tips (condensation in fine crevices is not predicted until at least 30% relative humidity), (ii) studies of SCC in thin foils using transmission-electron microscopy[9] show no evidence of dissolution and, (iii) fracture surfaces often show no signs of dissolution. In aluminium alloys, dissolution (e.g. of anodic grain-boundary precipitates) is probably important during crack growth at very low stress intensities (and during initiation of cracks), especially in 'corrosive' environments. Oxide-film formation, followed by fracture of films, probably also occurs when crack growth is slow (or discontinuous). In some cases, dissolution may occur **after** crack growth (e.g. by adsorption) and could influence subsequent cracking by changing solution chemistry (e.g. pH) at crack tips.

4.4.3 Hydrogen-Embrittlement

Embrittlement of materials (notably steels) by hydrogen has many similarities to LME[22] and many characteristics of hydrogen-embrittlement are consistent with a mechanism based on adsorption-activated nucleation of dislocations at crack tips. Observations of iron-alloy surfaces in hydrogen, using field-ion microscopy, do suggest that hydrogen facilitates nucleation of dislocations.[23]

In aluminium alloys, dry hydrogen gas does not induce sub-critical crack growth, and does not influence rates of fatigue-crack growth (where 'clean' surfaces at crack tips are certainly exposed to hydrogen).[24] These observations would be expected, on the basis of the previous discussion, since hydrogen molecules probably do not chemisorb on aluminium surfaces.[25] It has been suggested,[9] however, that SCC in aluminium alloys occurs as a result of the generation of hydrogen by the reaction between aluminium and water molecules, and the subsequent diffusion of hydrogen ahead of cracks which facilitates 'decohesion' across stressed grain boundaries. 'Hydrogen-embrittlement' theories of SCC in aluminium alloys have been based on (a) evidence that the embrittlement of tensile specimens by exposure to moist air during aging is

---

† This initial burst of rapid cracking is **sub-critical** crack growth induced by the environment since (i) the initial stress intensity is just below Kc and stress intensity decreases with increasing crack length in the specimens used, and (ii) similarly loaded specimens in water-vapour/air show only slow crack growth and, hence, the rapid fracture in aqueous solutions is probably not overload fracture initiated by the environment—e.g. by sharpening the crack tip.

due to diffusion of hydrogen into specimens,[8] (b) observations that specimens are more susceptible to SCC under tensile loading than under torsional loading[26] (testing mode, and the component of hydrostatic stress ahead of cracks, should not affect dissolution or oxidation at crack tips but should influence the concentration of hydrogen ahead of cracks), and (c) studies of SCC in thin foils[9]. These studies showed that (i) crack growth occurred along grain boundaries and along grain-boundary-precipitate/matrix interfaces—not in PFZ's, (ii) grain-boundary precipitates and matrix were not dissolved, and (iii) there was no evidence that plastic deformation had occurred during SCC.

The evidence for hydrogen-embrittlement of aluminium alloys, outlined above, is considered inconclusive since (a) the embrittlement of tensile specimens by aging in moist air could possibly be associated with intercrystalline pitting[27] (§4.2), and (b) the effect of stress-mode, and the thin-foil studies, are not inconsistent with SCC by adsorption-induced slip—the fact that dislocations were not observed adjacent to SCC in thin foils does not preclude slip processes since it is well known that dislocations can easily escape from foils. Moreover, the present results clearly show that plastic deformation occurs during SCC (Fig. 27); dimpled fracture surfaces (e.g. Fig. 16) also indicate that extensive deformation occurs in PFZ's during SCC. Other workers[27] have noted *areas* of dimples on fracture surfaces after SCC of Al-Zn-Mg alloys but they have usually attributed these areas to overload fracture of ligaments lagging behind the main crack front. While such an effect almost certainly occurs (cf. LME—Fig. 13), and probably accounts for larger-than-average dimples on fracture surfaces (Fig. 28), the observation that dimples cover almost all the fracture surface in some cases indicates that SCC itself results in dimples†. It should be noted that these observations were made for specimens given heat-treatment A ('wide' PFZ, 'small' area fraction of grain-boundary precipitates) which favours the formation of well defined dimples during crack growth. Nevertheless, SCC, (LME, and overload) in specimens with 'brittle' microstructures (e.g. narrow PFZ's and/or large area fractions of grain-boundary precipitates) probably also occur by slip, but often with insufficient general deformation ahead of cracks to nucleate voids. In this case, cracks would follow grain boundaries and grain-boundary-precipitate /matrix interfaces, fracture surfaces would be 'flat', and deformation associated with crack growth would be difficult to detect.

It is concluded that the experimental evidence, for aluminium alloys, favours a mechanism of SCC based on adsorption-induced nucleation of dislocations at crack tips rather than a dissolution or hydrogen-embrittlement process.

4.5 Effects of Microstructure, Environment and Stress Intensity on SCC in Al-Zn-Mg

The influence of microstructure on SCC can be understood to some extent in terms of a mechanism based on adsorption-induced slip at crack tips. The resistance of materials to both SCC and overload should largely be determined by the balance between crack growth and crack-tip blunting in relaxing elastic strain energy around cracks. Crack-tip blunting (and resistance to crack growth) should increase with (a) decreasing matrix strength, (b) decreasing area fraction of grain-boundary precipitates, and (c) increasing PFZ width (although PFZ width should have little effect if the area fraction of grain-boundary precipitates is large).[10, 11] These predictions are in general agreement with experimental observations[4]; e.g. the increased resistance to SCC conferred by overaging is probably related to the presence of more widely spaced grain-boundary

---

† Dimples on fracture surfaces after SCC generally are also smaller and shallower than those on overload fractures. The large, flat, equiaxed dimples (Figs 18, 19) are probably produced when voids nucleate some distance ahead of crack tips and grow slowly by creep (i.e. time-dependent thermally activated plastic flow) until intersected by the main crack front. These dimples are produced only in the intermediate stress-intensity range probably because, at high stress intensities (rapid crack growth), there is insufficient time for much void growth by creep; at low stress intensities, the stress is probably too low to produce significant creep. In inert environments, e.g. dry air (§3.2.4), creep processes alone are probably responsible for sub-critical crack growth. It has been reported that creep rates, in uncracked specimens, are accelerated by some environments and that adsorption is probably responsible[28]; thus, SCC could be considered as a creep process accelerated by adsorption.

precipitates and, to a lesser extent, to decreased matrix strength. (The *structure* of the interior of grains, e.g. whether precipitates are coherent or incoherent, should not be important.) Interpretation of the effect of changes in microstructure on SCC is usually difficult, and results of different studies may be apparently conflicting, since one variable cannot be changed independently of others; the influence of microstructure on SCC probably also depends on the environment and the stress intensity.

Environments which produce the greatest reductions in 'surface-lattice distortion' and, hence, the easiest nucleation of dislocations at crack tips, should produce the fastest rates of crack growth. As would be expected, liquid-metal environments (where both substrate and adsorbed atoms are metals) produce more rapid cracking than SCC environments (Fig. 1)†. Increased surface coverage by chemisorbed species should also facilitate crack growth since longer dislocation sources, probably requiring lower activation stresses, should then be able to operate. Aqueous and liquid-metal environments which rapidly produce dissolution of, or compound formation with, the base metal may not result in SCC or LME since environmental species may be chemisorbed for insufficient times to produce significant surface coverage by adsorbed species at a particular instant. (This could explain why some environments can cause intercrystalline corrosion but not SCC). The influence of environmental factors (e.g. electrode potential, pH) on rates of SCC could also occur because these factors influence adsorption.

The effect of stress intensity on rates of SCC (Fig. 1) is difficult to explain because many interacting variables are involved. Crack branching is often observed so that the *effective* stress intensity at crack tips is not known. The 'plateau' often observed at intermediate-to-high stress intensities probably arises because crack-growth rates are controlled by diffusion of environmental species to crack tips.[3]

5. CONCLUSIONS

1. Similarities, e.g. dimpled fracture surfaces between LME and SCC in Al-Zn-Mg, suggest that crack growth (in aluminium alloys and possibly other materials) in liquid-metal and SCC environments occurs by a common mechanism.

2. LME and SCC can be explained on the basis that chemisorption of environmental species facilitates nucleation of dislocations at crack tips.

3. Previously proposed mechanisms of LME (involving tensile separation of atoms at crack tips), and SCC in aluminium alloys (involving dissolution or hydrogen embrittlement) are not consistent with the present observations.

---

† The difference in type of adsorbed species between SCC and LME probably also explains why pure metals are embrittled by liquid-metal environments but are not generally susceptible to SCC.

REFERENCES

1. M. H. Kamdar, 'Embrittlement by Liquid Metals', Progress in Materials Science 1973, **15**, 289.

2. 'Fundamental Aspects of Stress-Corrosion Cracking', ed. R. W. Staehle, A. J. Forty and D. van Rooyen, NACE, 1969.

3. 'The Theory of Stress Corrosion Cracking in Alloys, ed. J. C. Scully, Publ. NATO, Brussels, 1971.

4. M. O. Speidel and M. V. Hyatt, 'Stress Corrosion Cracking of High Strength Aluminium Alloys', in Advances in Corrosion Science and Technology, vol. 2, p. 115, Ed. M. G. Fontana and R. W. Staehle, 1972.

5. R. W. Staehle, ref. 2, p. 7.

6. H. Nichols and W. Rostoker, 'Analogies between Stress Corrosion Cracking and Embrittlement by Liquid Metals', Trans. ASM, 1963, **56**, 494.

7. E. G. Coleman, D. Weinstein and W. Rostoker, 'On a Surface Energy Mechanism for Stress-Corrosion Cracking', Acta Met., 1961, **9**, 491.

8. L. Montgrain, G. M. Scamans and P. R. Swann, 'The Embrittlement of Al-Zn-Mg Alloys by Water', p. 194, 'The Third Tewksbury Symposium', ed. C. J. Osborn and R. C. Gifkins, Melbourne, 1974.

9. L. Montgrain and P. R. Swann, 'Electron Microscopy of Hydrogen Embrittlement in a High Purity Al-Zn-Mg Alloy', p. 575, 'Hydrogen in Metals', ed. I. M. Bernstein and A. W. Thompson, ASM, 1974.

10. S. P. Lynch, 'Tensile Deformation and Fracture in High Strength Al-Zn-Mg Alloys', Met. Sci. J., 1973, **7**, 93.

11. P. T. N. Unwin and G. C. Smith, 'The Microstructure and Mechanical Properties of Al-6% Zn-3% Mg', J. Inst. Metals, 1969, **97**, 299.

12. D. A. Ryder and A. C. Smale, 'A Metallographic Study of Tensile Fractures in Al-Cu and Al-Cu-Zn-Mg Alloys', p. 237, 'Fracture of Solids', ed. O. C. Drucker and J. J. Gilman, Interscience Publ., 1962.

13. P. C. Varley, M. K. B. Day and A. Sendorek, 'The Structure and Mechanical Properties of High Purity Al-Zn-Mg Alloys', J. Inst. Metals, 1958, **86**, 337.

14. C. A. Stubbington and P. J. E. Forsyth, 'A Comparison of the Fatigue Behaviour of Two Al-Zn-Mg Alloys', R. A. E. Tech. Report. No. 66201, 1966.

15. S. P. Lynch 'Mechanism of Liquid-Metal Embrittlement-Crack Growth in Aluminium Single Crystals and Other Metals in Liquid-Metal Environments', ARL, Mat. Report No. 102, 1977.

16. R. M. Latanision, 'Characterisation of Metal Surfaces', p. 185, 'Corrosion Fatigue;—Chemistry, Mechanics, and Microstructure', ed. O. F. Devereux, A. J. McEvily, and R. W. Staehle, Publ. NACE, 1971.

17. R. L. Fleisher, 'Effects of Non Uniformities on the Hardening of Crystals', Acta Met., 1960, **8**, 598.

18. H. H. Uhlig, 'Metal Surface Phenomena', p. 312, 'Metal Interfaces', American Society for Metals, 1952.

19. A. Kelly, 'Strong Solids', Clarendon Press, Oxford, 1973.

20. R. M. N. Pelloux, 'Crack Extension by Alternating Shear', Eng. Frac. Mech., 1970, **1**, 697.

21. R. M. N. Pelloux, 'Corrosion Fatigue Crack Propagation', p. 731, 'Fracture', Brighton, Chapman and Hall, 1969.

22. S. P. Lynch and N. E. Ryan, 'Mechanisms of Hydrogen Embrittlement—Crack Growth in a Low-Alloy Ultra-High Strength Steel Under Cyclic and Sustained Stresses in Gaseous Hydrogen', ARL Mat. Report No. 103, 1977, and 'Hydrogen in Metals' Paris, 1977, to be published.

23. J. A. Clum, 'The Role of Hydrogen in Dislocation Generation in Iron Alloys', Scripta Met., 1975, **9**, 51.

24. M. O. Speidel, 'Hydrogen Embrittlement of Aluminium Alloys?' p. 249, 'Hydrogen in Metals', ed. I. M. Bernstein and A. W. Thompson, ASM, 1974.

25. D. O. Hayward and B. M. W. Trapnell, 'Chemisorption', Butterworths, London, 1964.

26. J. A. S. Green, H. W. Hayden, and W. G. Montague, 'The Influence of Loading Mode on the Stress Corrosion Susceptibility of Various Alloy /Environment Systems', p. 200, 'Effect of Hydrogen on Behaviour of Materials', Ed. A. W. Thompson and I. M. Bernstein, Publ. Met. Soc. of AIME, 1975.

27. F. E. Watkinson and J. C. Scully, 'The Stress Corrosion Cracking of a High Purity Al-6% Zn3% Mg Alloy', Corrosion Science, 1972, **12**, 905.

28. R. W. Revie and H. H. Uhlig, 'Effect of Applied Potential and Surface Dissolution on the Creep Behaviour of Copper', Acta Met., 1974, **22**, 619.

FIGURES

EM — Electron-micrographs of secondary-carbon replicas

SEM — Scanning-electron micrographs

Arrows on micrographs indicate direction of crack growth.

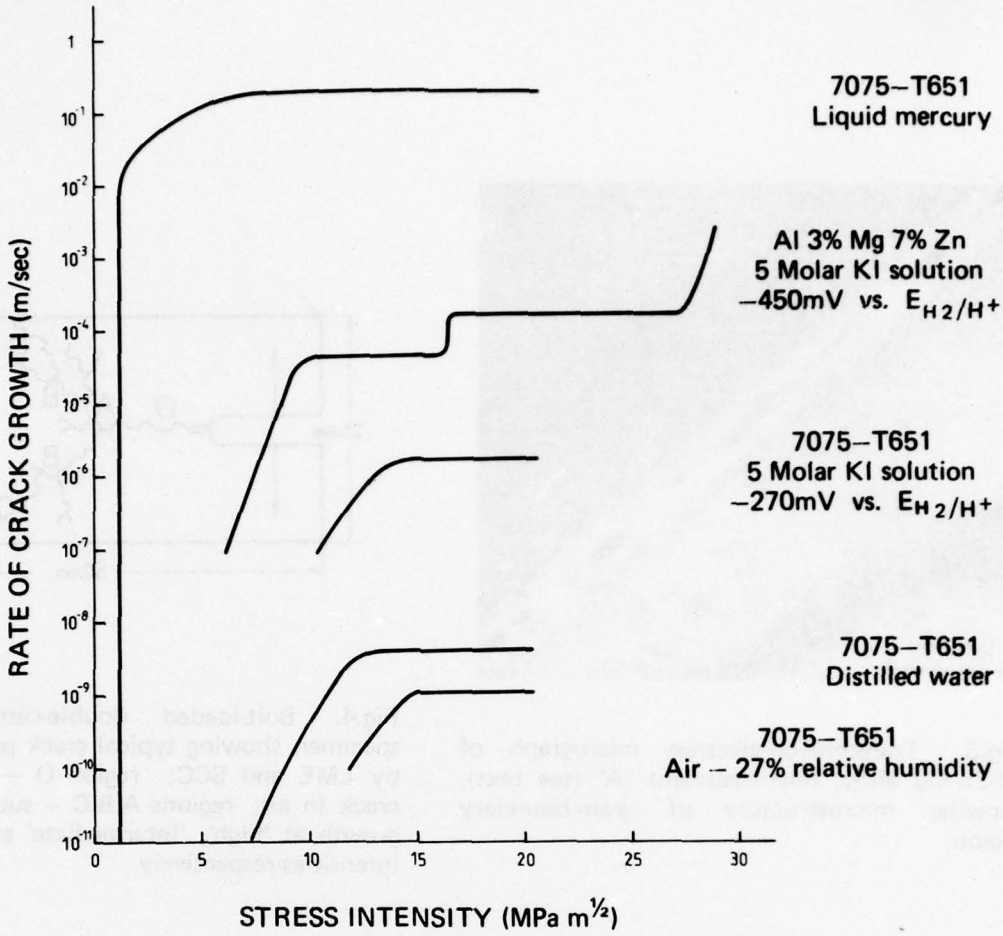

Fig.1. Graph showing variation in rate of sub-critical crack growth with stress intensity in different environments for aluminium alloys (Temperature 23°C, crack orientation TL for 7075 alloy) (replotted from data by Speidel (ref.4)).

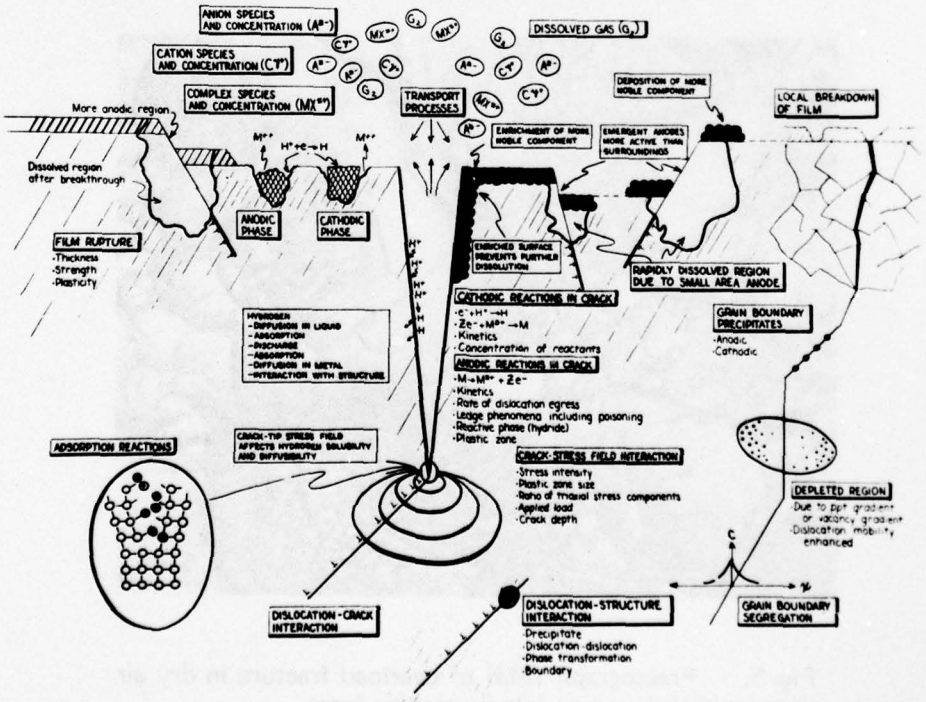

Fig.2. Montage showing processes which can influence SCC (after Staehle (ref.5)).

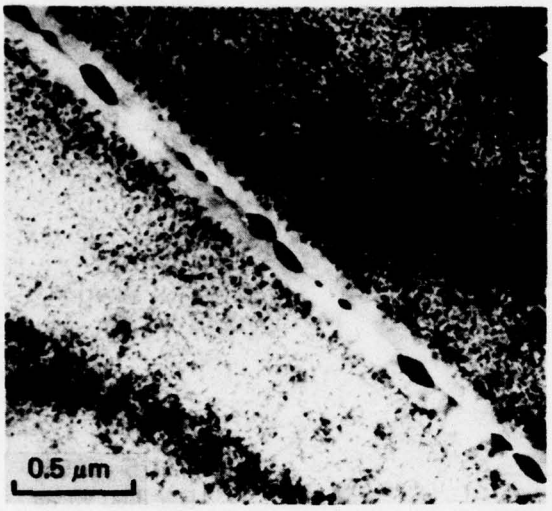

Fig.3. Transmission-electron micrograph of Al-Zn-Mg alloy, heat-treatment 'A' (see text), showing microstructure of grain-boundary region.

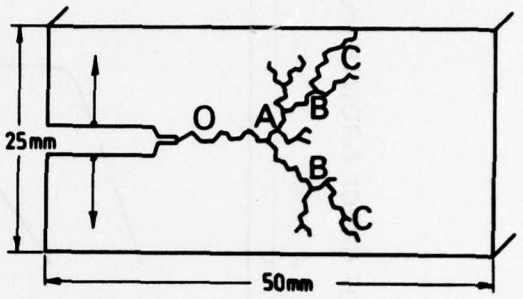

Fig.4. Bolt-loaded double-cantilever beam specimen showing typical crack paths produced by LME and SCC; region O – overload pre-crack in air; regions A,B,C – sub-critical crack growth at 'high', 'intermediate' and 'low' stress intensities respectively.

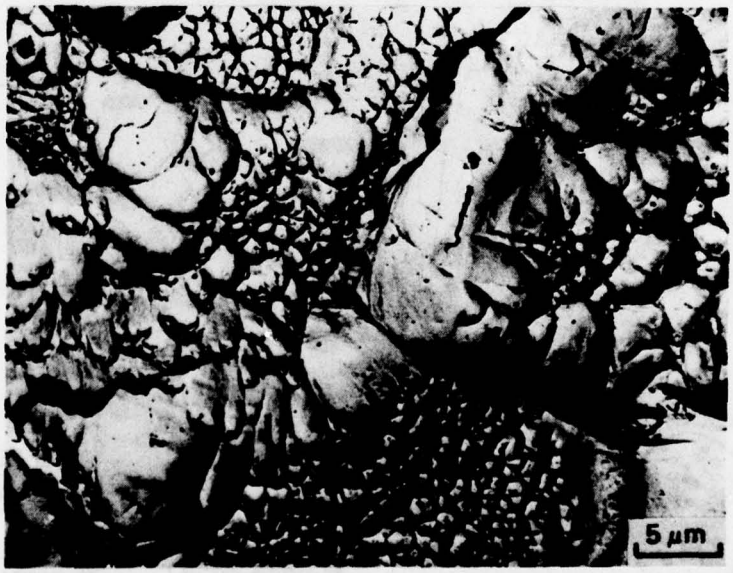

Fig. 5. Fractograph (EM) of overload fracture in dry air showing dimples on an intercrystalline facet.

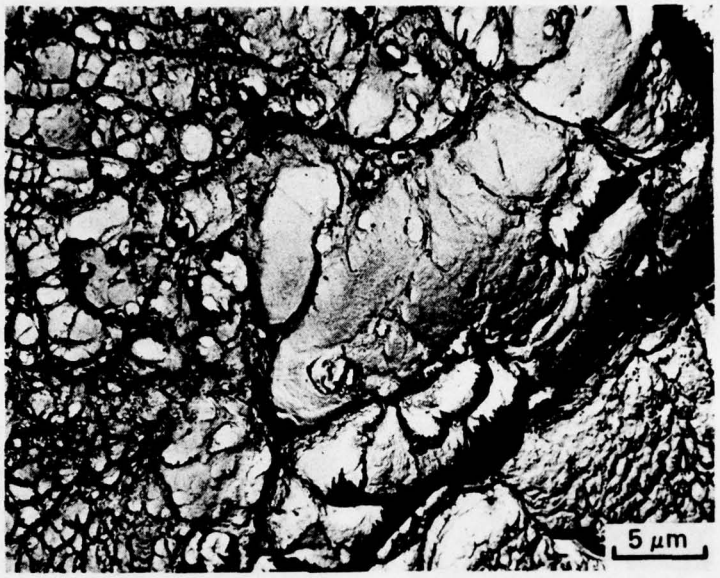

Fig.6.

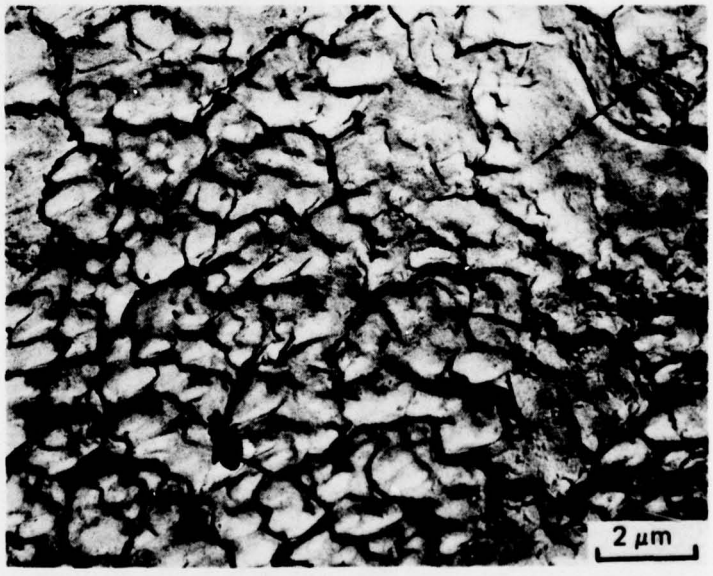

Fig.7.

Figs. 6,7. Fractographs (EM) after sub-critical crack growth induced by liquid mercury, at 'high' stress intensities, showing dimples, (slight oxidation of the fracture surface is evident in some regions, Fig.6)

Fig.8.

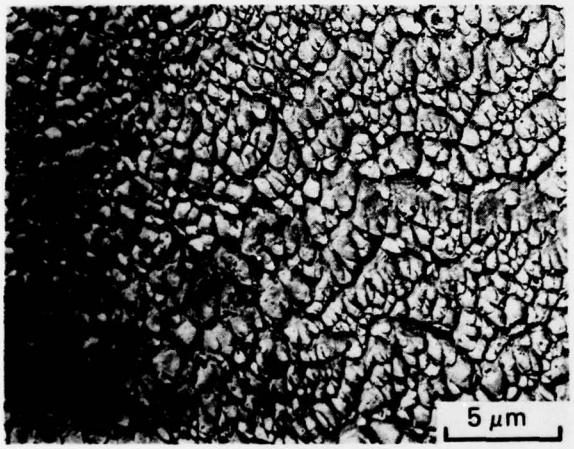

Fig.9.

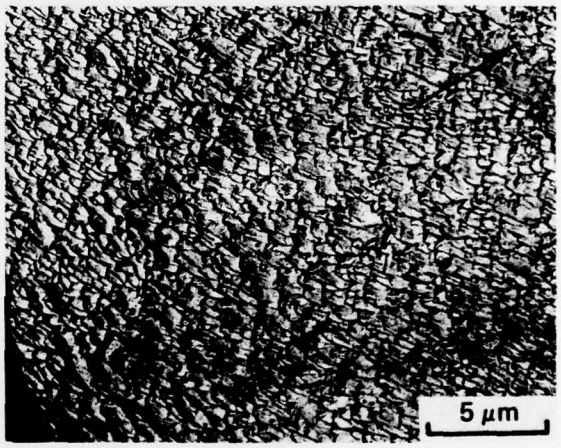

Fig.10.

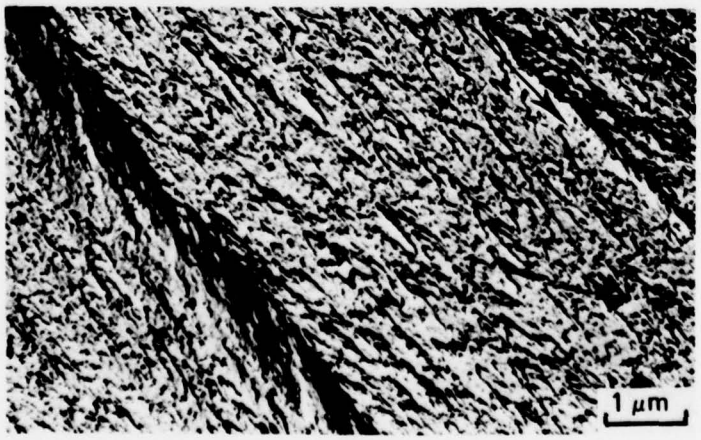

Fig.11

Figs.8 -11 Fractographs after sub-critical crack growth induced by liquid alloy showing dimples: Figs 8 (optical) and 9 (EM) – 'high' stress-intensity region; Fig.10 (EM) – 'intermediate' stress-intensity region and Fig.11 -- 'low' stress-intensity region. Dimples are smaller, shallower and more elongated at lower stress intensities.

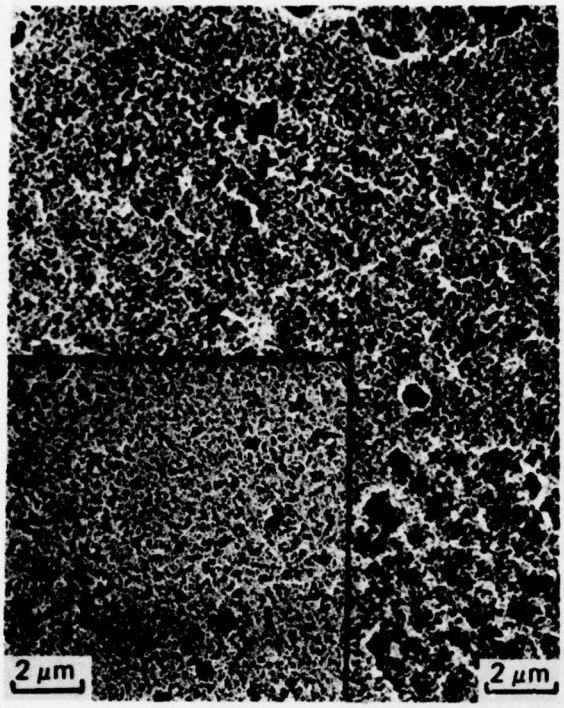

Fig.12. Electron micrographs (replicas) of electropolished surface of Al-Zn-Mg after 'fluxing' in NaOH solution, 'wetting' with liquid mercury (liquid alloy produced similar results), and then removing liquid mercury. Inset shows surface after immersion in NaOH solution only.

Fig.13. Fractograph (optical) after sub-critical crack growth induced by liquid alloy showing that most of the fracture surface is covered by a thin film of alloy and that small areas (light regions) had fractured without being 'wet' with liquid alloy.

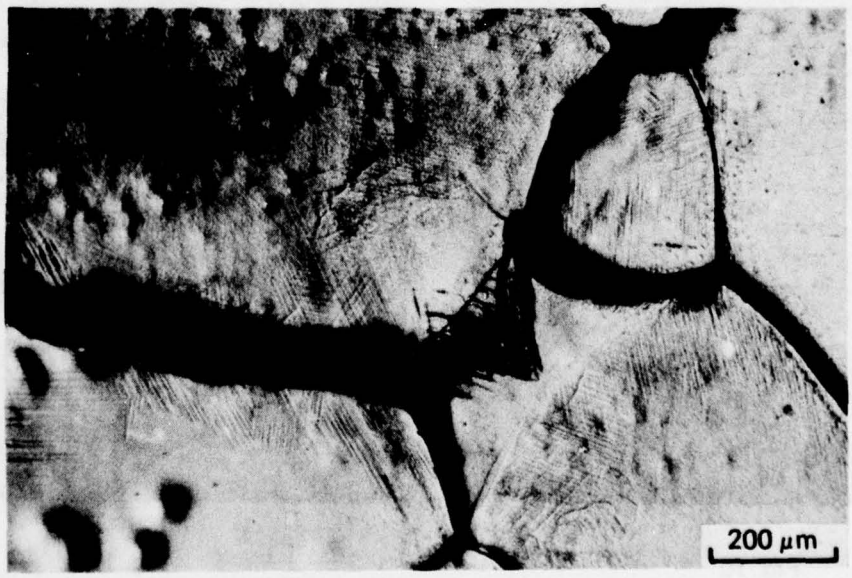

Fig.14. Optical micrograph (from the mid-section of a specimen) showing deformation, adjacent to cracks induced by liquid alloy, revealed by aging after fracture, sectioning, polishing and etching.

Fig. 15

Fig. 16

Fig. 17

Figs. 15 – 17. Fractographs showing that dimples are smaller and shallower after SCC (in distilled water at high stress intensities) than after overload fracture in dry air. Fig. 15 (optical) shows a transition from SCC to overload within one grain facet. Fig. 16 (EM) shows typical area after SCC and Fig. 17 (EM) shows typical region after overload fracture.

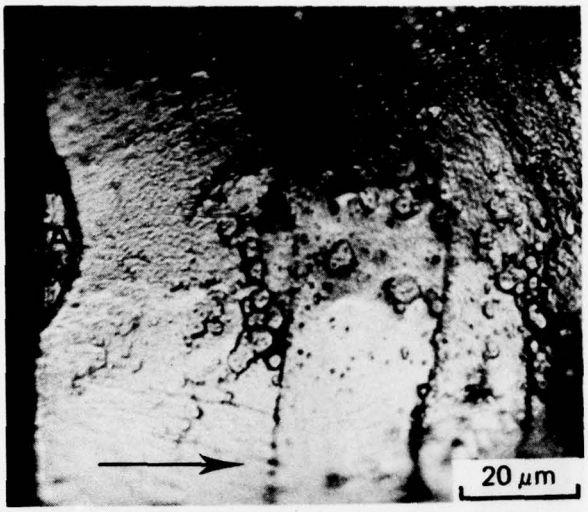

Fig.18.

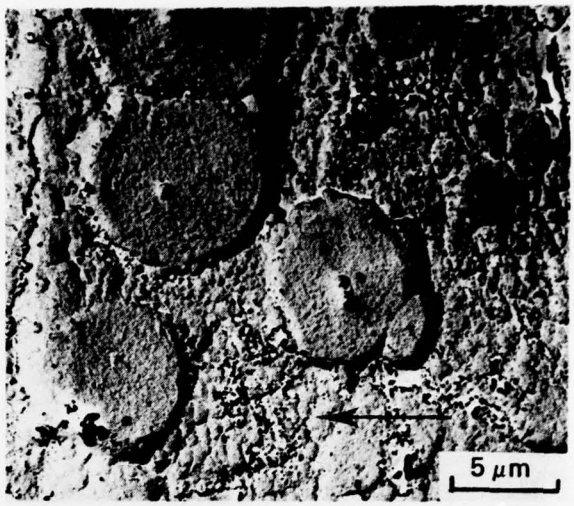

Fig.19

Fig.20.

Fig.21.

Figs.18–21. Fractographs (18,20 – optical, 19,21 – EM) after SCC in distilled water at 'intermediate' stress intensities showing large equiaxed dimples and areas of smaller dimples. Far left-hand side of Fig.18 is the edge (side surface) of the specimen; striations (crack-arrest markings) indicate that a crack has initiated from the surface (at A) ahead of the main crack and grown at right angles to the main crack front. Fig.20 shows steps, running approximately in the direction of crack growth, apparently initiated from large, equiaxed dimples.

Fig.22.

Fig.23.

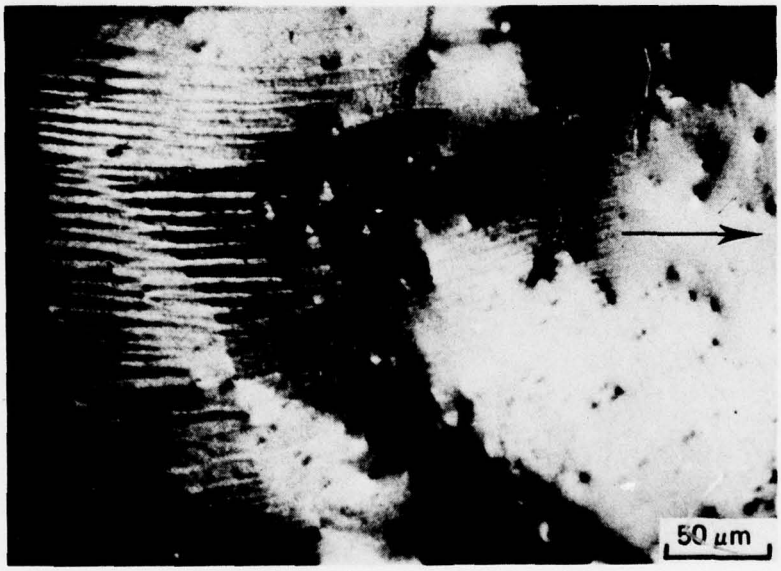

Fig.24.

Figs. 22 – 24. Optical fractographs (Fig. 24 – interference contrast) after SCC in distilled water at low stress intensities. Fig. 23 shows transition from SCC to overload fracture in dry air. SCC areas show apparently flat regions, isolated dimples, and slightly inclined steps running in the direction of crack growth.

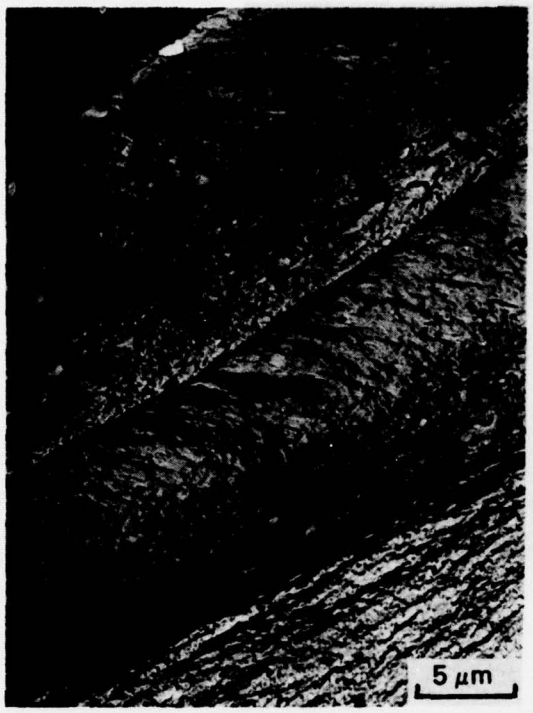

Fig.25.

Fig.26.

Figs. 25,26. Fractographs (EM) after SCC in distilled water at 'low' stress intensities revealing that very small, shallow, elongated dimples are present on facets similar to those shown in Figs. 22–24.

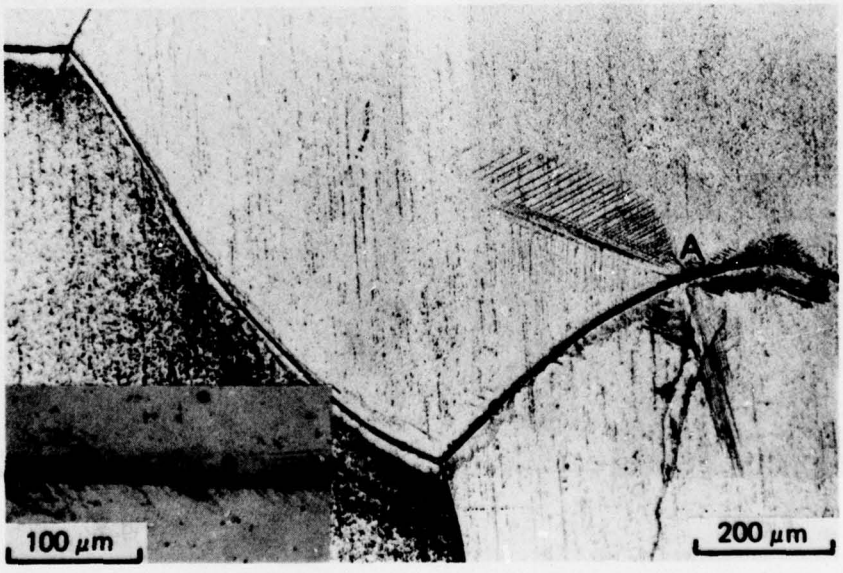

Fig.27. Optical micrographs showing deformation associated with SCC in distilled water at 'low' stress intensities (a) on previously electropolished side of specimen and (b) in mid-section, revealed by aging after fracture, sectioning, polishing and etching. The larger-than-average amount of deformation at A is probably associated with a period of crack-arrest/crack-tip blunting.

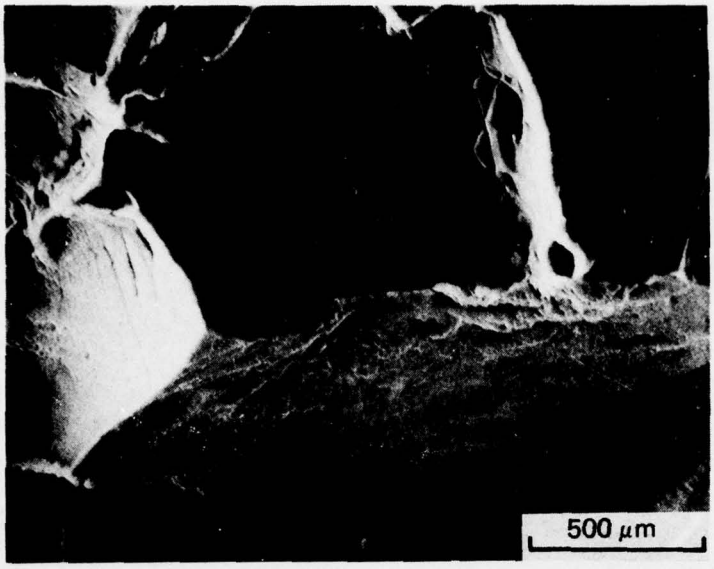

Fig.28.

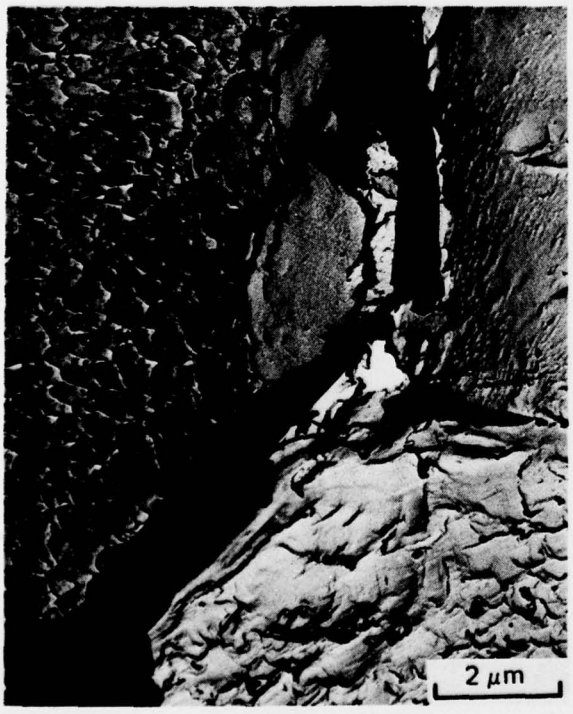

Fig.29.

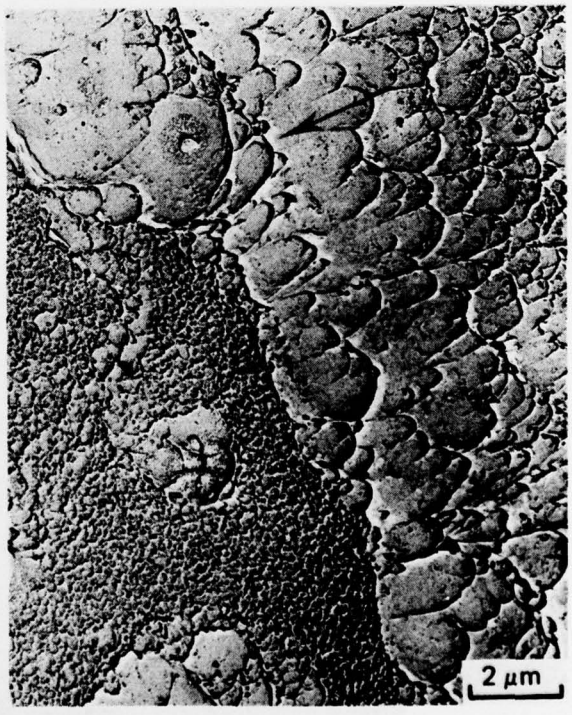

Fig.30.

Figs. 28–30. Fractographs (28–SEM; 29, 30–EM) after SCC in water-vapour/air (20% relative humidity) at 'high' stress intensities showing dimples on intercrystalline facets. Dimples were quite large in a few areas (Fig. 28) but were generally fairly small and shallow, and in some areas were only just resolved.

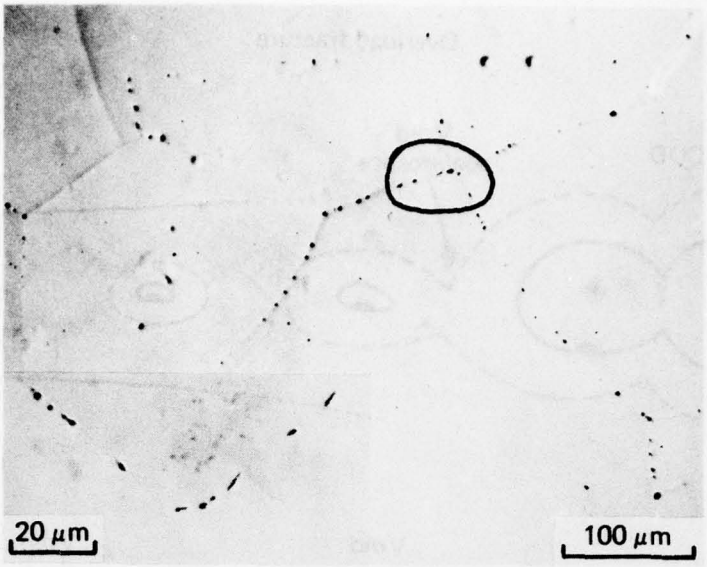

Fig. 31. Optical micrographs showing intercrystalline pitting/cracking produced by exposure of specimens to water-vapour/air (100% relative humidity) during aging for 4 days at 70°C; the original surface has been electropolished to remove ~ 4 μm. Inset shows circled region at higher magnification.

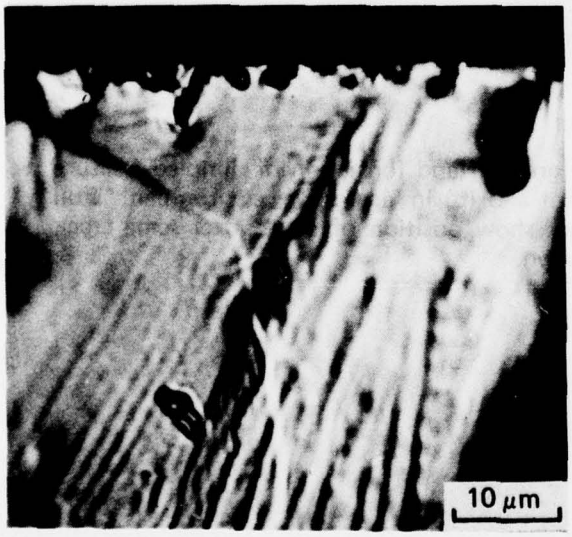

Fig.32.

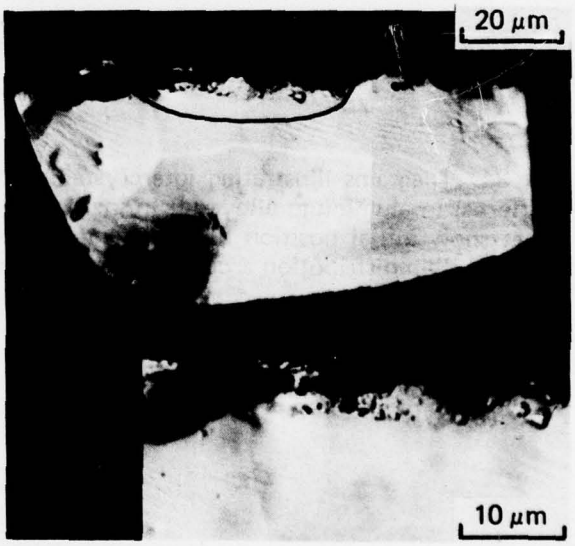

Fig.33.

Figs.32,33. Optical micrographs showing intercrystalline fracture surface of specimens exposed to water vapour/air during aging, then fractured in dry air. Pits extending into the specimen from the surface (see Fig.31) and small islands of a thin film close to the specimen surface have been 'sectioned' by the fracture. Inset (Fig.33) shows circled region at higher magnification.

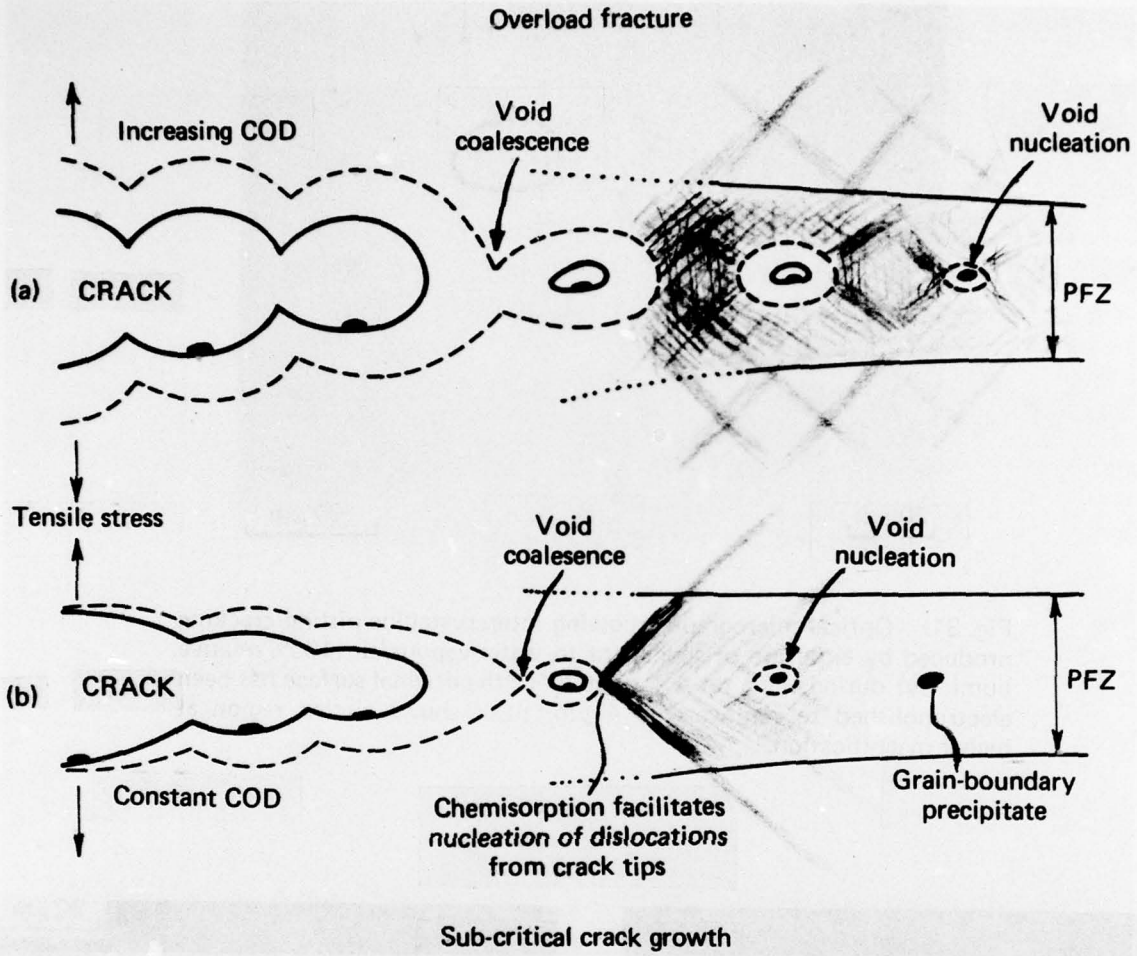

Fig.34. Diagrams illustrating intercrystalline crack growth (and formation of dimpled fracture surfaces) in aluminium alloys (a) in inert environment and (b) in 'aggressive' environment. Full lines show initial position of crack and dashed lines show position of crack after some crack growth. Slip distribution around crack tips is also shown.

DISTRIBUTION

Copy No.

AUSTRALIA

DEPARTMENT OF DEFENCE

Central Office

Chief Defence Scientist	1
Executive Controller, ADSS	2
Superintendent, Defence Science Administration	3
Defence Library—Campbell Park	4
Joint Intelligence Organization	5
Assistant Secretary, STIB	6–21

Aeronautical Research Laboratories

Chief Superintendent	22
Superintendent Materials Division	23
Divisional File Materials Division	24
Author—S. P. Lynch	25
Library	26

Materials Research Laboratories

Library	27

Weapons Research Establishment

Library	28

WITHIN AUSTRALIA

Australian Atomic Energy Commission, (Director), N.S.W.	29
C.S.I.R.O. Chief, Division of Tribophysics	30
C.S.I.R.O. Physical Metallurgy Division	31
Australian National Library	—

Universities

Monash	Library	32
	Professor I. J. Polmear	
Newcastle	Library	33
New England	Library	34
New South Wales	Physical Sciences Library	35

Royal Melbourne Institute of Technology

Library	36

CANADA

Department of Energy, Mines & Resources, (Dr A. J. Williams)	37
Library, Aluminium Laboratories	38

FRANCE

A.G.A.R.D., Library 39
O.N.E.R.A. 40

GERMANY

Deutsche Versuchsanstalt fur Luft and Raumfahrt 41

INDIA

Ministry of Defence, Aero. Development Est. 42
Indian Institute of Science, Library 43
Indian Institute of Technology, Library 44
National Aeronautical Laboratory (Director) 45
C.A.A.R.C. Co-ordinator Materials: Dr. S. Ramaseshan 46

JAPAN

Tohoku (Sendai) University, Library 47

NETHERLANDS

N.L.R. (Director), Amsterdam 48
N.L.R. R.J.H. Wanhill 49

NEW ZEALAND

Air Department, R.N.Z.A.F., Aero. Documents Section 50
Department of Civil Aviation, Library 51
University of Canterbury, Library 52

SWEDEN

Aeronautical Research Institute 53

UNITED KINGDOM

Australian Defence Scientific and Technical Representative 54
Aeronautical Research Council, N.P.L. (Secretary) 55
C.A.A.R.C., M.P.L. (Secretary) 56
Royal Aircraft Est., Library, Farnborough 57
Royal Aircraft Est., Library, Bedford 58
Royal Armament Research & Development Est., Fort Halstead 59
Aircraft and Armament Experimental Est. 60
Military Engineering Experimental Est. 61
Motor Vehicles Experimental Est. (Director) 62
National Engineering Labs. (Superintendent), Scotland 63
The British Library, Science Reference Library (Holborn Divn.) 64
Central Electricity Generating Board (Dr. I. Mogford), Leatherhead 65–66
Metals Abstracts, Editor 67
Rolls-Royce (1971) Ltd, Aero. Divn., Chief Librarian, Derby 68

Universities

Birmingham	Dr. J. Beevers, Dept. of Physical Metallurgy & Science of Materials	69
Bristol	Dr. W. J. Plumbridge, Mech. Eng.	70
Cambridge	Dr. J. Knott, Metallurgy & Materials Science Dept.	71
Manchester	Dr. G. Lorimer, Metallurgy Dept.	72

Manchester (Inst. of Sci. and Tech.)	Mr. D. A. Ryder, Metallurgy Dept.	73–74
Imperial College	P. R. Swann Dept. Metallurgy & Materials Science	75
Leeds	J. C. Scully, Metallurgy Dept.	76
Newcastle	R. N. Parkins, Metallurgy Dept.	77

UNITED STATES OF AMERICA

Counsellor Defence Science	—
N.A.S.A. Scientific & Information Facility, College Park	78
Naval Air Systems Command, Dept. of Navy, Mr. R. Schmidt	79
A.R.C. Westwood, Martin Marietta Labs, Baltimore, Md.	80

Universities

Prof. R. W. Staehle, Dept. Metallurgical Engineering, Ohio State Univ.	81

Institutes of Technology

Illinios (Memorial Inst.)	Prof. E. N. Pugh, Dept. Metallurgical Engineering	82
Massachusetts	R. M. N. Pelloux	83
Prof. N. S. Stoloff	Rensselaer Polytechnic Institute, New York	84

Spares	85–95